TOWARDS THE VALIDATION OF NEUTRON NOISE SIMULATORS: QUALIFICATION OF DATA ACQUISITION SYSTEMS

A. Rais[1], V. Lamirand[1,5], O. Pakari[1], A. Laureau[1], J. Pohlus[2],
C. Pohl[3], S. Hübner[4], M. Hursin[1,5], C. Demazière[6], A. Pautz[1,5]

[1]Laboratory for Reactor Physics and Systems Behaviour, EPFL, Lausanne, Switzerland
[2]Institute for Safety Technology, TÜV Rheinland ISTec GmbH, Hallbergmoos, Germany
[3]TÜV Rheinland ISTec GmbH, Cologne, Germany
[4]Faculty of Mechanical Science and Engineering, TUD, Dresden, Germany
[5]Nuclear Energy and Safety Research Division, PSI, Villigen, Switzerland
[6]Chalmers University of Technology, Göteborg, Sweden

ABSTRACT

This paper deals with the processes involved in the generation of reliable experimental data for the validation of computer simulations. In the field of neutron noise, the analysis of results is based on spectral features of the detector signals in the frequency domain. Neutron noise simulators also produce estimates that are subjected to studies in the same domain. The validation process of such simulations begins with the generation of reliable experimental data. In this work, we analyze results from two neutron noise experimental campaigns. The focus is placed upon de comparison of results obtained by different data acquisition systems (DAQs) that were used to record the data in parallel. The goal is to verify whether results obtained by the different DAQs are consistent, and thus reliable.

The neutron noise-dedicated experiments were carried out in the AKR-2 reactor at the Technische Universität Dresden and in the CROCUS reactor at the École polytechnique fédérale de Lausanne. The experiments consisted in introducing different types of periodic reactivity perturbations: a rotating neutron absorber with a varying absorption cross-section with respect to the rotation angle; a linearly vibrating absorber that is moved back and forth inside the reactor core; and a fuel rods oscillator that allows to vibrate a set of fuel rods.

KEYWORDS: CORTEX, CROCUS reactor, AKR-2 reactor, neutron noise

1. INTRODUCTION

The fluctuation of the signals obtained from the neutron detectors in a nuclear reactor are often referred to as neutron noise. These fluctuations arise from the intrinsic stochasticity of the neutron chain and from perturbations in the macroscopic cross-sections such as due to the vibration of mechanical components inside a reactor.

The analysis of these fluctuations is precisely the subject of this work which has been carried out as part of the CORTEX project (CORe monitoring Techniques and EXperimental validation

and demonstration). CORTEX has been funded by the European Commission under the Horizon 2020 framework and aims at developing an innovative core monitoring technique to detect nuclear reactor anomalies at a very early stage. This would allow nuclear utilities to take proper actions before such problems have any adverse effect on plant safety and reliability.

Since the CORTEX project targets the development of high-fidelity methods, their validation represents an essential part of the project. This process has began with the generation of noise-specific experimental data from two zero-power facilities: the AKR-2 reactor at Technische Universität Dresden (Germany) and in the CROCUS reactor at the École polytechnique fédérale de Lausanne (Switzerland). Because different data acquisition systems (DAQs) were simultaneously used to record the experimental data, the consistency of results from the different DAQs needs to be verified in order to ensure data reliability.

This paper is structured as follows: the first section introduces the neutron noise experiments carried out at the AKR-2 and CROCUS reactors, the second section focuses on the comparative assessment of results obtained by three different DAQs, and the last section provides some highlights and the conclusions of this work.

2. DESCRIPTION OF NEUTRON NOISE EXPERIMENTS

The experiments presented here were specifically designed for the validation of neutron noise simulations and were carried out using two different nuclear facilities: the AKR-2 and CROCUS reactors.

The AKR-2 reactor [1] is a thermal, homogeneous, polyethylene moderated zero-power reactor with an allowed maximum power of 2 Watt. The core has cylindrical shape with a diameter of 250 mm and a height of 275 mm, and is surrounded by a 32 cm thick layer of graphite reflector. The disk-shaped fuel elements consist of a homogeneous dispersion of polyethylene and uranium oxide (19.8 % enriched). The biological shield consists of two cylindrical walls of thickness 15 cm and 58 cm made of paraffin and heavy concrete, respectively as illustrated in Figure 1a.

The CROCUS reactor [2] is an uranium-fueled and light water-moderated zero-power reactor with an allowed maximum power of 100 Watt. The core is approximately cylindrical in shape with a diameter of about 58 cm and a height of 100 cm. The active core region is partially submerged in water, and the water level is allowed to vary to control the core reactivity. The reactivity can also be controlled by means of two control rods containing boron carbide pellets. There are two different kinds of fuel rods: the central zone is loaded with 336 UO_2 fuel rods (1.806 % enriched), which are arranged in a square lattice of 1.837 cm pitch. The peripheral zone is loaded with 176 thicker, U_{metal} fuel rods (0.947 % enriched) with a lattice pitch of 2.917 cm.

Two different sources of reactivity perturbations were used in the AKR-2 reactor. These perturbations induce neutron flux fluctuations that were measured by different neutron detectors. The first type of perturbation is generated by a rotating neutron absorber that has a varying absorption cross-section with respect to the rotation angle. The rotating absorber shaft was inserted in the
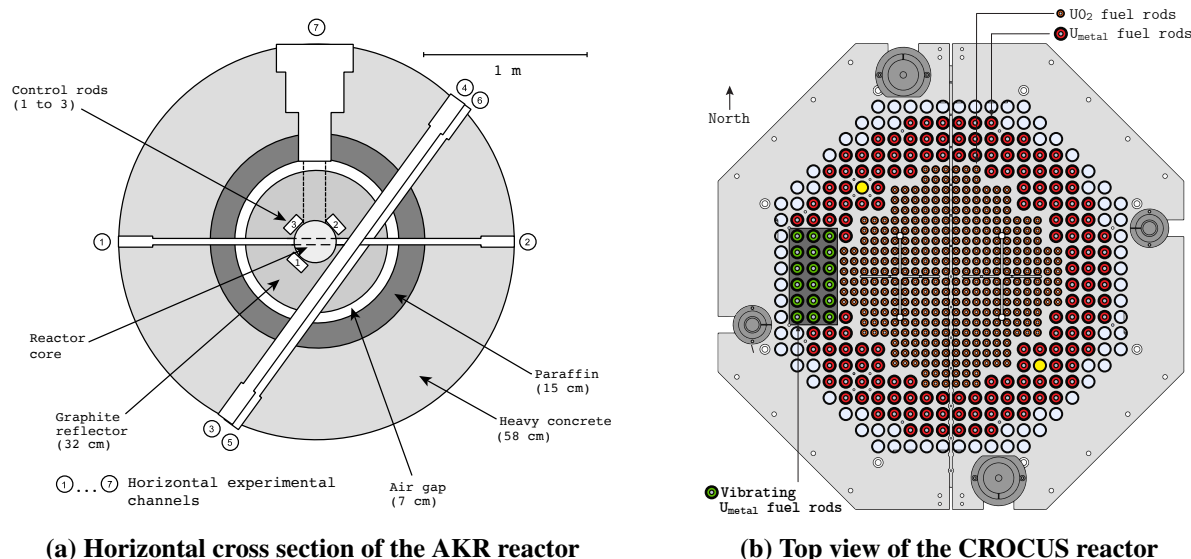
(a) Horizontal cross section of the AKR reactor

(b) Top view of the CROCUS reactor

Figure 1: The AKR-2 and CROCUS zero-power reactors

tangential experimental channel 3-4 which is shown in Figure 1a. The second type of perturbation is generated by a linearly vibrating absorber that is moved back and forth inside the reactor core along the experimental channel 1-2. The neutron flux levels were measured by seven different ex-core detectors, and the signal readout and storage was performed by three independent DAQs. Details about these data acquisition systems are provided in Section 3.

The experiments in the CROCUS reactor consisted in oscillating 18 of the metallic uranium fuel (U_{metal}) rods laterally (west-east direction) as illustrated in Figure 1b. These experiments were carried out within the framework of the COLIBRI experimental program [3] that was specifically developed for that purpose. The COLIBRI in-core device consists in two moving plates located above and below the core grids, and rigidly connected by an aluminum beam. Each moving plate is attached to an extremity of the 18 fuel rods, which allows to oscillate the set of fuel rods. The nuclear instrumentation consists of 11 detectors comprising reactor operation and safety monitors together with several ex-core and in-core detectors [7]. The detectors' signal readout and storage was performed simultaneously by several independent DAQ in an analogous manner than in the AKR-2 experiments.

Details about the AKR-2 and CROCUS experimental campaigns will be available in a companion publication [4].

3. QUALIFICATION OF DATA ACQUISITION SYSTEMS

The different data acquisition systems used in the AKR-2 and CROCUS experiments were supplied by the TUD, EPFL, and the Institut fur Sicherheitstechnologie GmbH (ISTec). The ISTec data acquisition system, referred to as SIGMA, is highly specialized in measuring noise signals deriving from neutron flux density fluctuations. The SIGMA module measures voltage signals provided by neutron detectors with an amplitude range of ± 10 Volts. Depending on the detector type and counting rate, the original pulse or current signals are converted to voltage signals by detector spe-
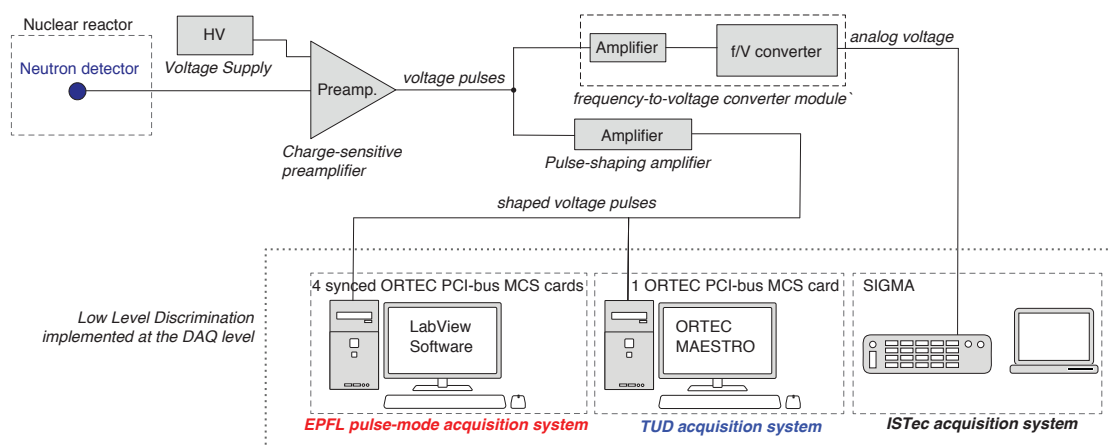
Figure 2: Neutron detection sequence and DAQs used in the AKR-2 experiments

cific preamplifiers, and in the case of pulse signals by an additional frequency-to-voltage-converter. This frequency-to-voltage-converter filters frequencies higher than 2 Hz. The EPFL pulse mode acquisition system comprises four synchronized PCI-based multichannel-scalers (from ORTEC) which have the ability to store up to 65 thousand data points and sample at a maximum of 150 MHz. The acquisition is controlled by in-house developed LabVIEW routines. In addition to the pulse mode DAQ, EPFL employs a Lecroy Wavesurfer 10 oscilloscope that was used as current mode DAQ [5,**?**] for the CROCUS experiments. Finally, the TUD acquisition system is similar to that one from EPFL (ORTEC MCS-pci) except that it uses a single PCI-card and is based on the MAESTRO acquisition software developed by ORTEC.

Figure 2 shows a scheme of the electronics associated with the detection chain used in the AKR-2 experiments. This figure shows that the detection sequence is similar for EPFL and TUD systems but different for the ISTec case because of the frequency-to-voltage-converter. These differences may have an impact in the comparison as it will be later discussed.

Figure 3 shows an scheme of the electronics associated with the current-mode detection chain used in the CROCUS experiments that are compared in this work.
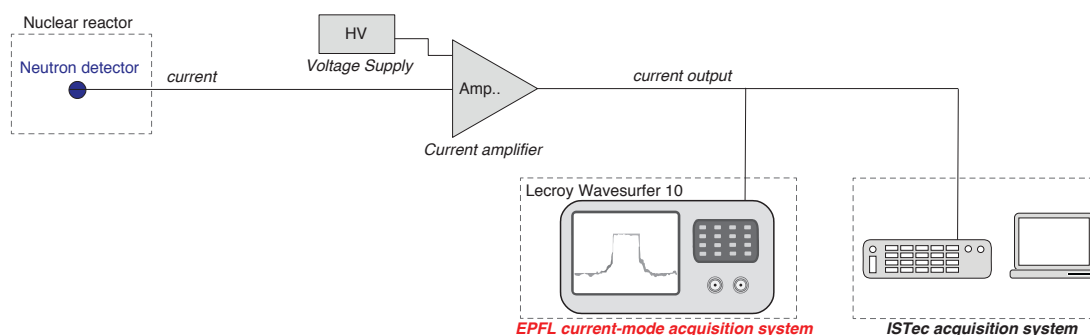

Figure 3: Neutron detection sequence and DAQs used in the CROCUS experiments

The DAQs' qualification focuses on the comparison of experimental results in the frequency domain. When we deal with a power density spectrum, the main peak amplitude (corresponding to

the fundamental frequency) is an indicator of how much weight this frequency will contribute to the overall signal power, and thus was chosen as the parameter for the comparison of data acquisition systems. Because the signals are subjected to various sources of noise that are distributed throughout the frequency spectrum, the comparison in terms of peak amplitudes is meaningful. The ISTec DAQ (SIGMA) was chosen as the reference for the comparison as it has been qualified for industrial applications.

Prior to computing the peak amplitudes, several steps were required to process the signals obtained from the three data acquisition systems. These steps consisted first in synchronizing the three signals and secondly in standardizing the data by subtracting the mean value of the signal and normalizing with respect to the signals' standard deviation. The power density spectra were computed using the periodogram method which is given by:

$$P_{xx} = \frac{2\,|FTT(x)^2|}{f_s N} \tag{1}$$

where $FTT(x)$ is the Fast Fourier Transform of the signal x, f_s is the signal sampling frequency and N the number of signal data points. The frequency is an array of size $N/2$ that goes from zero to $f_s/2$, with a frequency resolution of $\Delta f = f_s/N = 1/t_f$, where t_f is the total sampling time. It is therefore important to note that, for a fixed total sampling time t_f, increasing the sampling rate will not impact on the frequency resolution, it will rather increase the signal's bandwidth (i.e,, resolve larger frequencies).

The amplitude of the peak corresponding to the fundamental frequency was found by searching for the maximum peak value in the power density spectrum for frequencies larger than 0.1 Hz. The cutoff frequency of 0.1 Hz was set because in some cases the amplitude at lower frequencies exceeds that one of the main peak.

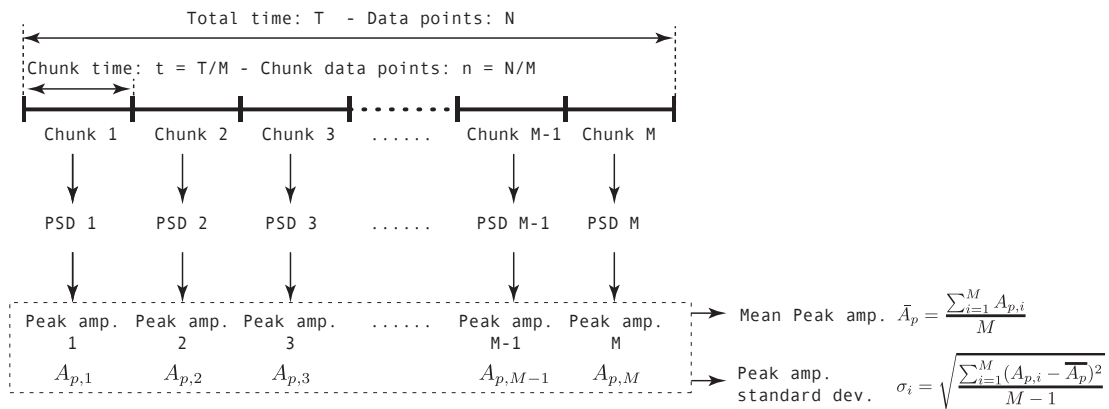### 3.1. Uncertainty quantification on peak amplitude estimate

Figure 4: Uncertainty quantification process for peak power estimation

The signals acquired during the experiments presented in this work carry information from two main sources of fluctuations. The first fluctuation source results from the induced perturbation and thus is the one of interest for its accurate identification. The induced perturbation fluctuations

will be hereafter referred to as *signal*. The second fluctuation source is given by the inherent stochasticity of the neutron chain. Because these fluctuations are practically random and contain no useful information for this analysis, they will be referred to as *unwanted noise*. An additional source of *unwanted noise* may arise from the detection systems electronics.

The estimation of parameters from the power density spectrum is subjected to uncertainties related to the acquisition time and the unwanted noise (i.e. stochastic fluctuations). A small reactivity perturbation in the reactor will result in a time series with low signal-to-(unwanted) noise ratio and thus, resolving the fundamental frequencies will require longer acquisition times than the large perturbation counterpart. Because the uncertainties are related to the signal's unwanted noise, for a fixed time length, the uncertainties are expected to be higher in the case of small perturbations.

The process for quantifying the uncertainty is schematized in Figure 4 and relies on slicing the signal (from any DAQ) in M smaller chunks. Next, the PSD for each chunk is estimated using the method described above, and each power density spectrum (PSD) is later used to compute M peak amplitudes.

The figure of merit for evaluating benchmark results is the z-score defined as:

$$z = \frac{\overline{A_{p,x}} - \overline{A_{p,ISTec}}}{\sqrt{(\sigma_{i,x})^2 + (\sigma_{i,ISTec})^2}} \tag{2}$$

where $\overline{A_{p,ISTec}}$ and $\sigma_{i,x}$ are the mean peak amplitude and standard deviation from EPFL (or TUD) data.

It is worth noting that the scaling factor M should not be arbitrarily chosen. A very small M factor provides good estimation of each individual chunk peak amplitude ($A_{p,i}$), but a small sample size for estimating the standard deviation (σ_i). On the other hand, a large M factor provides good statistics for the standard deviation, but a low frequency resolution ($\Delta f = M \cdot f_s / N$) and thus a weaker estimate of the peak amplitude. An investigation of the impact of the choice of M over the z-scores has been performed to show that the benchmarking results shown below (computed
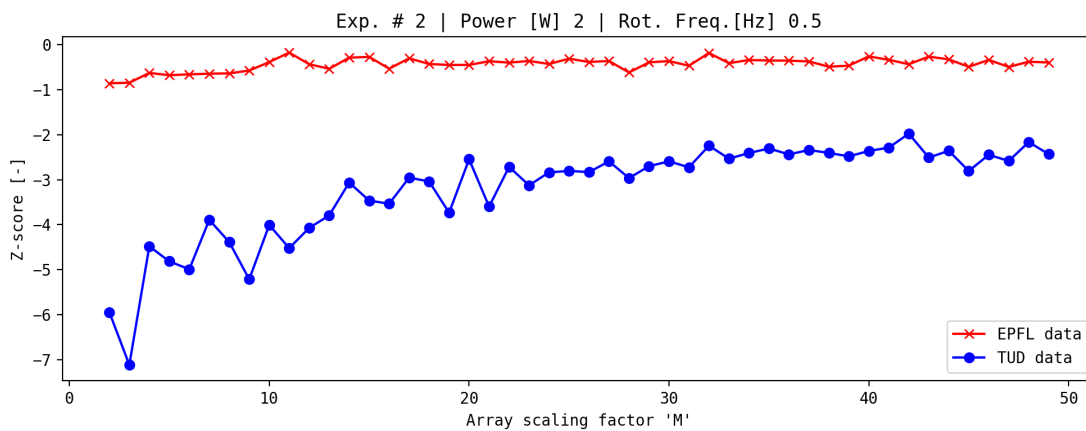

Figure 5: EPFL and TUD z-scores a function of M scaling factor. Measurement no. 2.

with a fixed M value) do remain confined after certain value of M. Figure 5 shows the z-score as a function of M for the rotating absorber experiment. A value of M = 32 was chosen to compute the peak amplitudes reported in the results section. A fixed value of M means that, in each experiment, a fixed 'chunk' acquisition time has been considered for the uncertainty e stimation. Because the total acquisition length varies from experiment to experiment, the 'chunk' acquisition length also varies with each experimental run.

3.2. AKR-2 results

The comparison between the three DAQs for the AKR-2 campaign is only possible for signals from one detector (det. # 1) because the TUD system recorded data for this detector only. A typical power density spectrum corresponding to the AKR-2 rotating absorber experiments is shown in Figure 6.
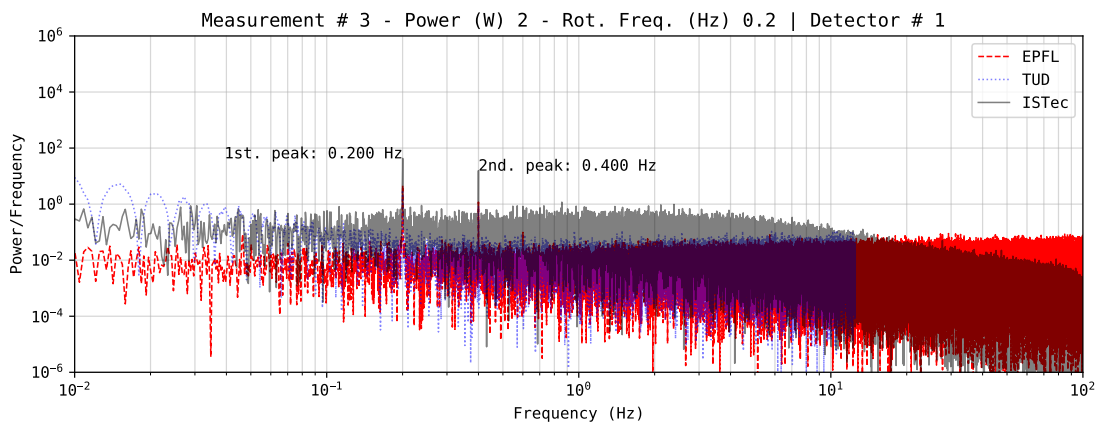

Figure 6: Power spectra for rotating absorber measurement no. 3. AKR-2 detector 1

The results of the DAQs comparison are expressed in terms of relative peak amplitudes and associated uncertainties (normalized with respect to the ISTec value: $A_{p,x}/A_{p,ISTec}$) and also in terms of z-scores, where the ISTec DAQ is the reference (recall Equation 2). Figure 7 shows the results for each measurement, where measurements 1 to 10 correspond to the rotating absorber experiments and 11 to 27 to the vibrating absorber experiments. The measurement cases where only EPFL results are reported imply that no data was measured by TUD acquisition system. Figure 7 shows the large differences in uncertainty levels between the rotating absorber (1 to 10) and vibrating absorber experiments (11 to 27). These differences are associated to the fact that the magnitude of the induced perturbation is much lower for the rotating absorber experiments, thus these signals carry weaker signal-to-unwanted-noise ratios that lead to higher uncertainties.

The z-score results from Figure 7 indicate that EPFL and TUD peak amplitudes estimates are comparable to those obtained with the ISTec reference system as the z-scores are enclosed, for the most part, by the $2\sigma_c$ band, where σ_c stands for the combined uncertainty (root of sum squares). Usually, an absolute value of the z-score below 2 indicates satisfactory performance, between 2 and 3, questionable performance, and above 3 unsatisfactory performance. Note that an essential reason for having achieved good agreement is that uncertainties are large in relative terms (in the order of tens of percent). These uncertainties are dependent on the acquisition length, correspond
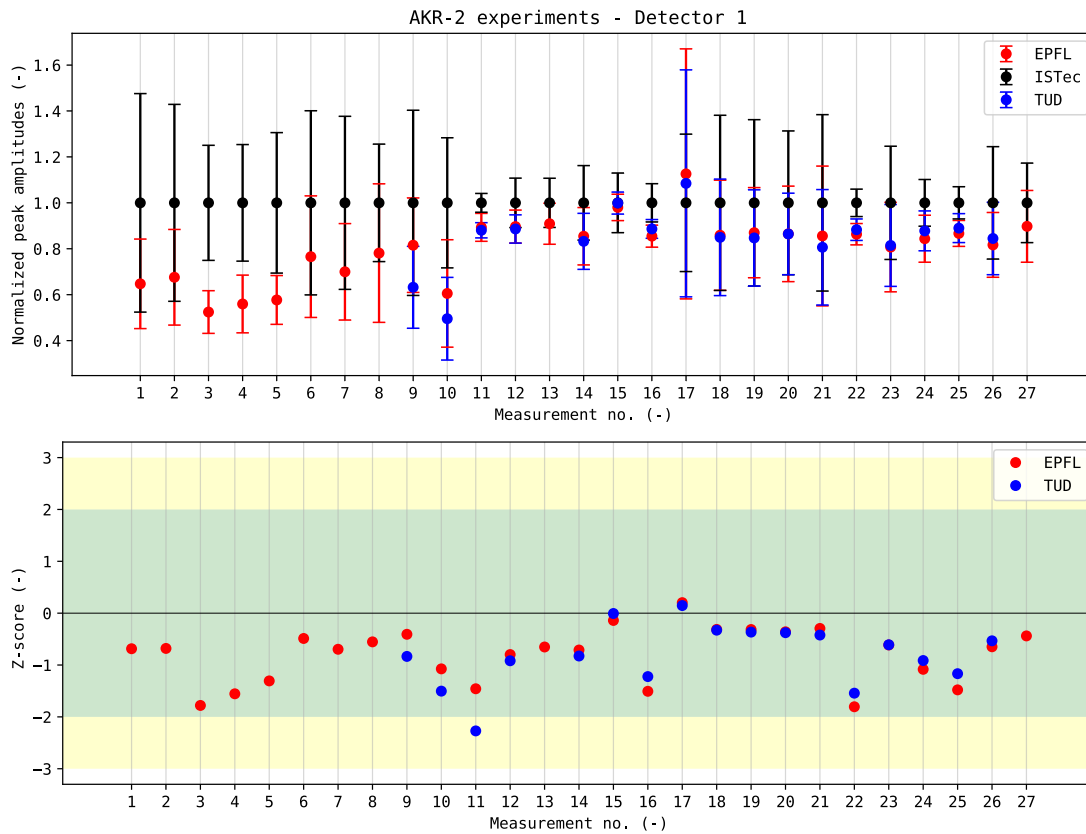
Figure 7: Results for AKR-2 experiments. Pulse-mode acquisitions

only to a fixed 'chunk time', and shall not be extrapolated to other acquisition lengths. Longer acquisition times (or 'chunk times') would allow to lower the uncertainty levels and thus to better resolve differences between DAQs.

Figure 7 also reveals at first sight, the presence of a bias, given that the EPFL and TUD z-scores are, in most cases, negative. This bias can be explained by the fact that the reference signal (ISTec) passes through a frequency-to-voltage-converter (see Fig. 2) that filters out frequencies higher than 3 Hz and thus the contribution of these higher frequencies to the normalized power (integrated PSD) is much lower than for EPFL and TUD DAQs. This leads to higher ISTec peak amplitudes that can be clearly seen in Figure 6. The link between the bias and the frequency-to-voltage-converter was verified with the results for the CROCUS campaign (Section 3.3) where ISTec and EPFL DAQs are compared for current signals (i.e. the frequency-to-voltage-converter is not required) and no bias is revealed.

3.3. CROCUS results

For the CROCUS campaign, the comparison was done for current mode acquisition and therefore TUD DAQ was not included in the comparison. Note that the electronics associated with the detection are not the same than that one used in the ARK-2 experiments (see Fig. 3).

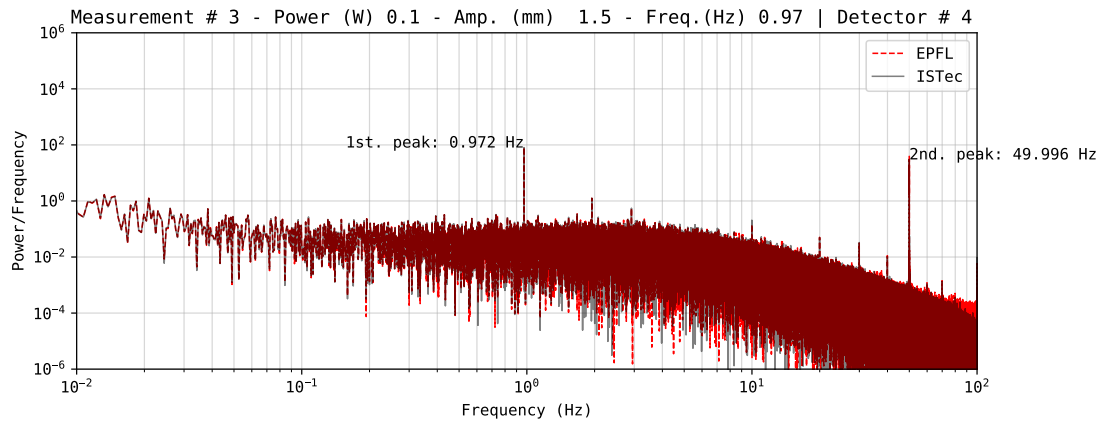A typical power density spectrum corresponding to the CROCUS vibrating fuel experiments is

Figure 8: Power spectra for vibrating absorber measurement no. 3. CROCUS detector 4

shown in Figure 8, where the fuel rods were vibrating at 0.97 Hz with an amplitude of ± 1.5 mm. Note that the amplitude response in the upper extreme of the frequency domain is consistent with the presence of an anti-aliasing low pass filter within the ISTec DAQ with a cutoff frequency of 100 Hz.
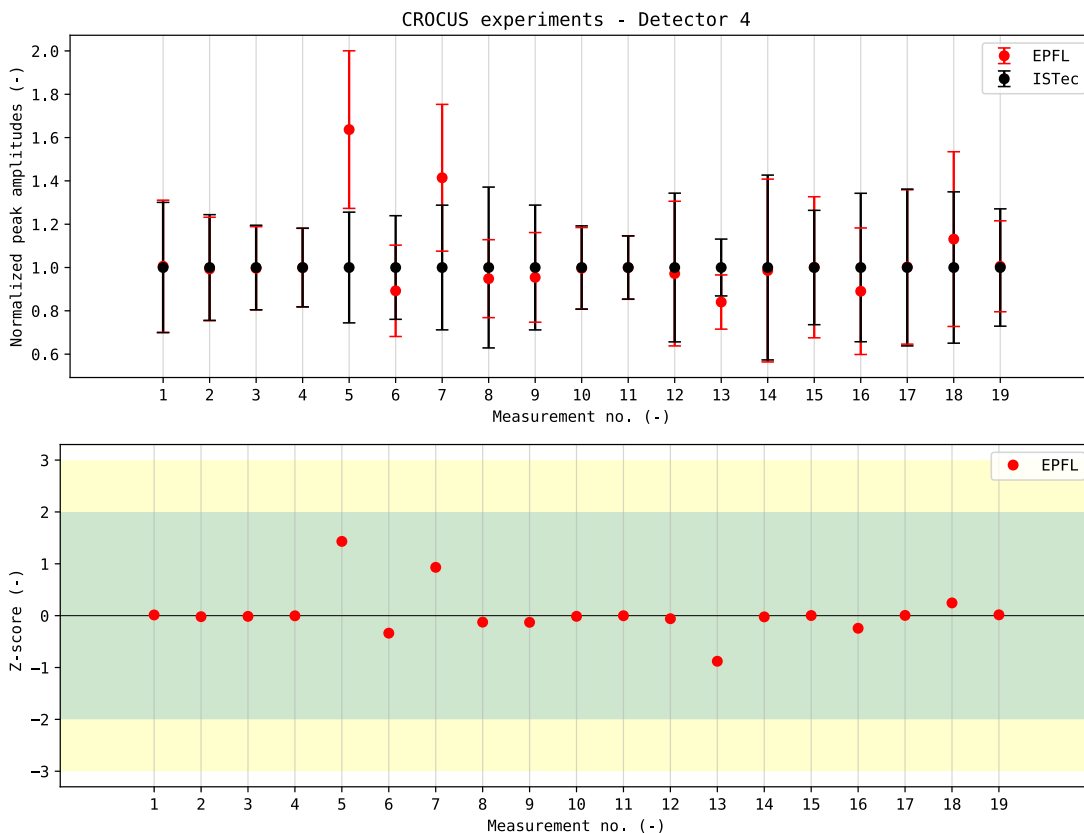

Figure 9: ISTec and EPFL results for CROCUS experiments. Current-mode acquisitions

The results are again expressed in terms of relative peak amplitudes (normalized with respect to the ISTec value: $A_{p,x}/A_{p,ISTec}$), and also in terms of z-scores. The z-score results from Figure 9

indicate that EPFL peak amplitudes estimates are in excellent agreement with those obtained with the ISTec reference system as most z-scores are contained within the $1\sigma_c$ band. In addition, these results indicate that, for this level of uncertainties, no bias is exposed. However, as explained for the AKR-2 experiments, the good level of agreement is due to the large uncertainties that prevents resolving differences between DAQs.

4. CONCLUSIONS

The comparison of data acquisition systems for the AKR-2 experiments revealed the presence of a bias that results from the different electronics used by the data acquisition systems. More precisely, the bias would be caused by the frequency-to-voltage converter used by the ISTec DAQ, and not by the other two DAQs. In addition, even though the TUD and EPFL DAQs are essentially identical, differences between their results can be attributed to the assignment of different low level discriminator values that eliminate all incoming voltage pulses (or energies) that are lower than that level.

The comparison of data acquisition systems for the CROCUS experiments shows better agreement as compared to the AKR-2 experiments. These results also verify that the omission of the frequency-to-voltage converter (used by ISTec for the AKR-2 experiments) reduces the bias observed in the AKR-2 experiments comparison.

Even though the results presented in this comparative study are dependent on the acquisition time (chunk times used for the uncertainty quantification), they represent an upper bound of the differences we can find for longer acquisition times. Accordingly, longer acquisition times would allow to better resolve differences because the uncertainty levels would be lower. Overall, it is safe to conclude that, for the given acquisition times, both EPFL and TUD acquisition systems can accurately reproduce the results obtained by the ISTec reference system.

REFERENCES

[1] "Technical Description and Procedure of Operation for the Reactor Facility AKR-2" *Technische Universität Dresden*, 2015.

[2] Früh, R, "Réacteur CROCUS, Complément au rapport de sécurité: Réactivité et paramètres cinétiques" *École polytechnique fédérale de Lausanne*, 1993.

[3] Lamirand, V., et al. "Future experimental programmes in the CROCUS reactor" *Conference proceedings of RRFM/IGORR 2016*. No. EPFL-CONF-218310. 2016.

[4] Lamirand, V., et al. "Neutron noise experiments in the AKR-2 and CROCUS reactors for the CORTEX European project" *in proceedings ANIMMA conference 2019*, 17-21 June 2019, Portorož, Slovenia.

[5] Pakari O., et al. "Current mode neutron noise measurements in the zero power reactor crocus." *In EPJ Web of Conferences*, volume 170, page 04017. EDP Sciences, 2018.

[6] Pakari, O., et al. "Kinetic Parameter Measurements in the CROCUS Reactor Using Current Mode Instrumentation." *IEEE Transactions on Nuclear Science* 65.9 (2018): 2456-2460

[7] Pakari, O., et al. "Investigation of spatial effects on neutron noise measurements in the zero power reactor CROCUS." *In proc. PHYSOR conference*, 2018.